THE JOURNAL OF PHYSICAL CHEMISTRY Letters

pubs.acs.org/JPCL

Letter

Structure of Furin Protease Binding to SARS-CoV-2 Spike Glycoprotein and Implications for Potential Targets and Virulence

Naveen Vankadari*

Cite This: J. Phys. Chem. Lett. 2020, 11, 6655−6663

Read Online

ACCESS | Metrics & More | Article Recommendations | Supporting Information

ABSTRACT: The COVID-19 pandemic is an urgent global health emergency, and the presence of Furin site in the SARS-CoV-2 spike glycoprotein alters virulence and warrants further molecular, structural, and biophysical studies. Here we report the structure of Furin in complex with SARS-CoV-2 spike glycoprotein, demonstrating how Furin binds to the S1/S2 region of spike glycoprotein and eventually cleaves the viral protein using experimental functional studies, molecular dynamics, and docking. The structural studies underline the mechanism and mode of action of Furin, which is a key process in host cell entry and a hallmark of enhanced virulence. Our whole-exome sequencing analysis shows the genetic variants/alleles in Furin were found to alter the binding affinity for viral spike glycoprotein and could vary in infectivity in humans. Unravelling the mechanisms of Furin action, binding dynamics, and the genetic variants opens the growing arena of bona fide antibodies and development of potential therapeutics targeting the blockage of Furin cleavage.

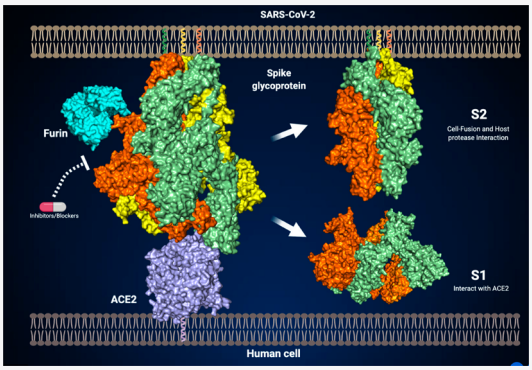

The pandemic corona virus disease 2019 (COVID-19) caused by severe acute respiratory syndrome coronavirus 2 (SARS-CoV-2) is an urgent public health emergency and is having serious impacts on global health.[1] To date, more than 620000 deaths and 15 million confirmed positive cases have been reported globally, making it the most contagious pandemic in the past decade (www.coronavirus.gov). SARS-CoV-2 is an enveloped single-strand, positive-sense RNA coronavirus, and its genome length of 29 kb is "hypothesized" to have transmitted form bats. The mutations and genetic changes in the SARS-CoV-2 continue to increase,[2] making containment of the virus difficult. Since the initial reporting of this pneumonia-causing novel coronavirus (SARS-CoV-2) in Wuhan, China, mortality and morbidity have increased exponentially globally despite several antiviral and antibody treatments.[3] Several antiviral drugs targeting different host and viral proteins have been clinically evaluated and repurposed to combat SARS-CoV-2 infection; neutralizing antibodies targeting the SARS-CoV-2 spike glycoprotein are the most frequently used.[3,4] In several major clinical studies, patients were prescribed with drugs such as remdesivir (to block RdRp), arbidol (impede spike protein), and ritonavir and hydroxychloroquine (unknown target).[5,6] However, infection control continues to be extremely challenging, with global case numbers increasing exponentially (www.cdc.gov). COVID-19 is a serious concern and warrants a detailed understanding of the molecular and structural features of SARS-CoV-2 structural proteins under native conditions and post-viral infection. This will improve our understanding of the dynamics and mechanism of viral action on the human cell.

In this regard, several epidemiological and evolutionary reports have highlighted several unique sequence deletions and insertions in the SARS-CoV-2 genome compared to previously known SARS, MERS, and bat coronavirus.[7,8] The viral spike glycoprotein is essential for host cell adhesion via ACE2 and CD26 receptors.[9−11] Among the various genetic variations, insertion of a Furin protease cleavage site in the spike glycoprotein (amino acids 682−689) is strikingly novel in SARS-CoV-2[12−14] (Figure S1) and related to enhanced virulence. This insertion was not found in other related coronaviruses (SARS-CoV-1, bat-CoV, and Pangolin-CoV), but MERS contains a pseudo-binding site (Figure 1A). Furin protease belongs to the family of calcium (Ca^{2+})-dependent proprotein/prohormone convertases (PCs) that are ubiquitously expressed in humans, and its levels are significantly elevated in lung cystic fibrosis.[15] Furin protease also cycles among the trans-Golgi network (TGN), the cell membrane (viral attachment), and endosomes (viral translocation in the endosomes). Furin recognizes the R-X-K/R-R motif and cleaves the peptide in the presence of Ca^{2+}[16,17] and is also known for cleaving different viral (influenza and HIV) envelope glyco-

Received: June 1, 2020
Accepted: July 28, 2020
Published: July 28, 2020

ACS Publications © XXXX American Chemical Society

https://dx.doi.org/10.1021/acs.jpclett.0c01698
J. Phys. Chem. Lett. 2020, 11, 6655−6663

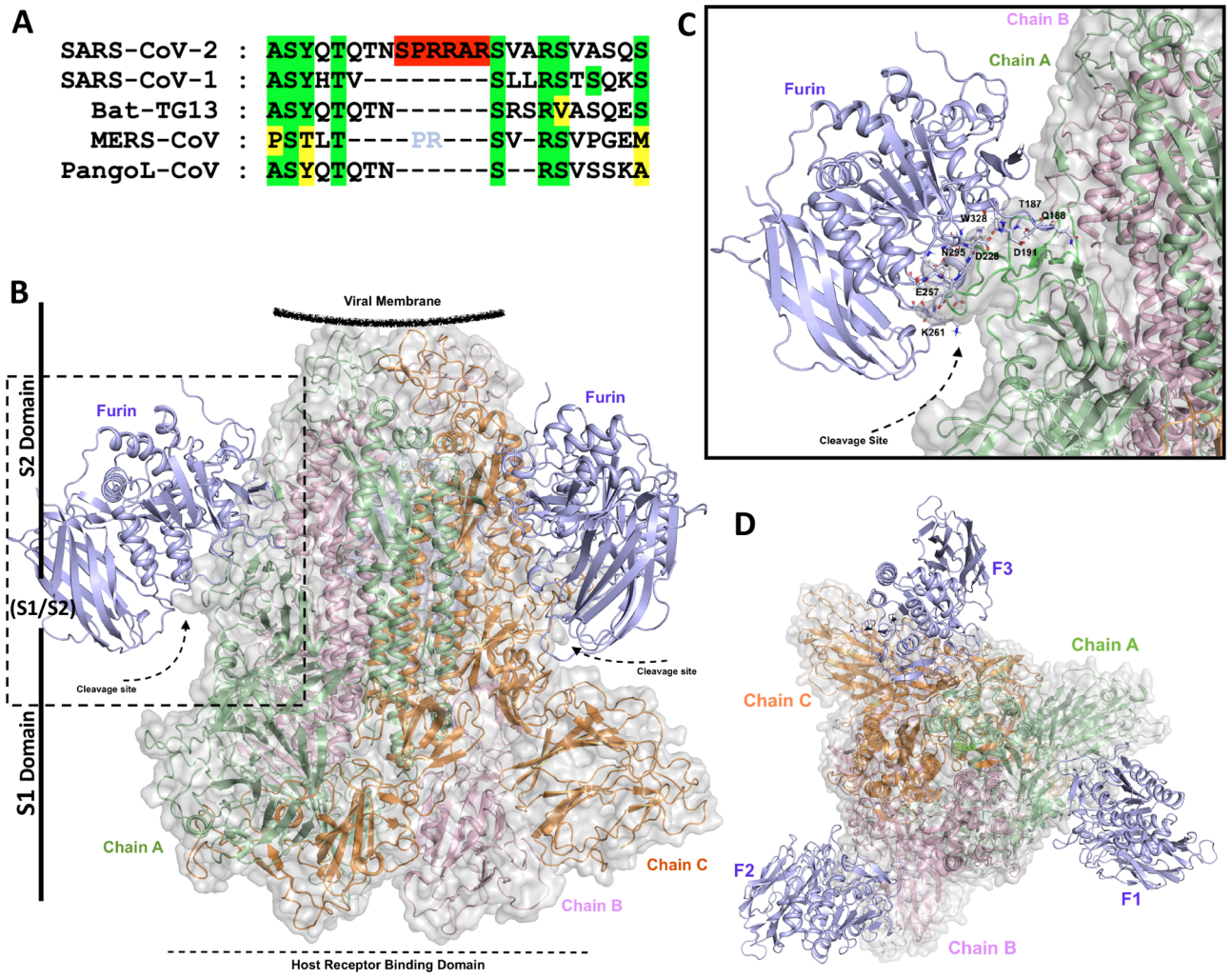

Figure 1. (A) Multiple-sequence alignment of the different coronavirus spike proteins. Identical amino acids are highlighted in green, similar amino acids in yellow, and unique Furin cleavage site amino acids in red. (B) Overall structure showing the SARS-CoV-2 spike glycoprotein homotrimer (substrate unbound or closed conformation) in complex with human Furin protease. The three monomers of the SARS-CoV-2 spike glycoprotein homotrimer are colored green (chain A), pink (chain B), and orange (chain C), and the docked Furin protease is colored blue. The spike protein cleavage site is indicated by the arrow, and the S1 and S2 domains are labeled. (C) Close-up showing the single Furin interacting with its target cleavage site (loop) of SARS-CoV-2 spike glycoprotein. Color coding and labeling are the same as for panel B. (D) Top view of panel A. Three Furin proteases at the adjoining conformation in the S1/S2 region of spike protein can be seen.

proteins, thereby enhancing fusion of the virus with the host cell membrane.[17−19] However, it is unclear whether Furin can bind and act on viral spike glycoproteins to cleave the spike glycoprotein and is directly related to enhanced virulence. Furthermore, it is important to understand the host genetic variants and mutation in Furin and its correlation with a differential viral infection. Hence, understanding the mode of interaction and mechanism of action between Furin and spike glycoprotein warrants further structural and biomolecular studies to understand the viral mechanism of action and for the development of bona fide therapeutics (drugs and antibodies).

To better understand the structural and molecular mode of interactions between SARS-CoV-2 spike protein and human Furin, we first undertook structural studies using molecular dynamics and computational model-based selective docking and simulation of SARS-CoV-2 spike glycoprotein in complex with Furin protease. To this end, we used a previously published and validated model structure of full-length SARS-CoV-2 spike glycoprotein[10] refined and modeled over the cryo-EM structure [Protein Data Bank (PDB) entry 6VSB][20] and a published structure of human Furin (PDB entry 1P8J or 1JXH).[16] The root-mean-square deviation (RMSD) of the previously published model structure and cryo-EM structure was 0.84, which suggests overall structural accuracy even with Furin cleavage sites. With these individual structures, we used three independent servers, Cluspro protein−protein docking (www.cluspro.bu.edu), Frodock (http://frodock.chaconlab.org/), and HADDOCK (https://haddock.science.uu.nl/), for further validation and determination of the precision of the docking mode and interaction (Figure S2). Among the five tentative clusters, cluster 1 of the docked complex shows the highest HADDOCK score, a larger reproducible cluster size, and the lowest possible RMSD, suggesting the high likelihood of the true structure. This confidence was also further enhanced by the observed lowest binding free energies in cluster/model 1, which makes us consider it for selecting the best possible model (Figure S2B−E). Further validation and refinement were completed by ensuring that the residues occupied Ramachandran-favored positions using Coot (www.mrc-imb.cam.uk/).

https://dx.doi.org/10.1021/acs.jpclett.0c01698
J. Phys. Chem. Lett. 2020, 11, 6655−6663

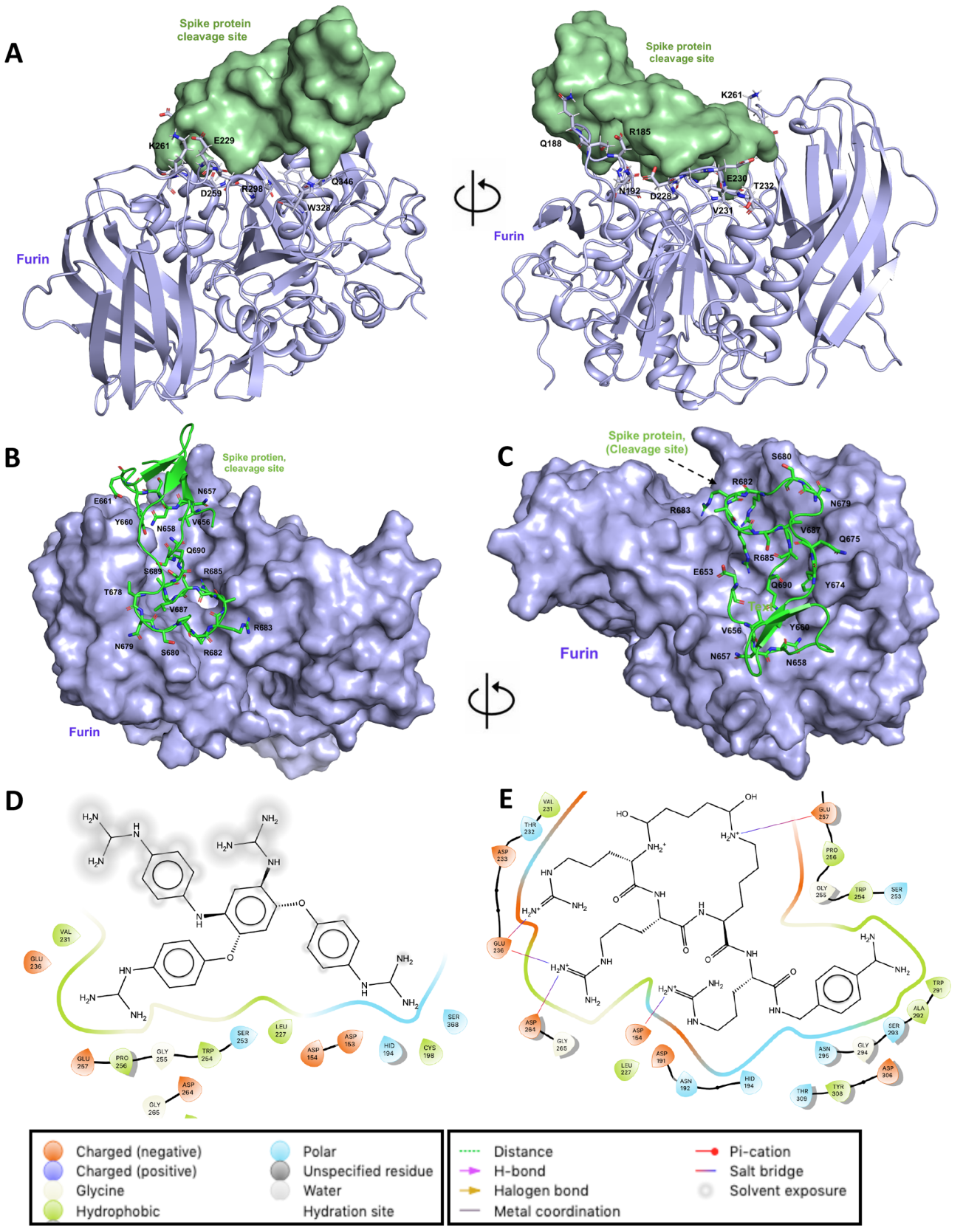

Figure 2. Surface and cartoon representation showing the detailed amino acid interaction between the Furin protease and SARS-CoV-2 spike glycoprotein. (A) Front and orthogonal views of Furin (blue sticks and cartoon) interacting with the target S1/S2 cleavage site of SARS-CoV-2 spike glycoprotein (green surface). The key residues of Furin involved in the interaction with the S1/S2 cleavage site are shown as sticks and labeled. (B and C) Front and orthogonal views of Furin (blue surface) interacting with the SARS-CoV-2 spike glycoprotein (green sticks). For clear visualization, one Furin-binding loop is shown. The canyon-like crevice is distinguishable in Furin, and the side chin residues of spike protein are labeled. (D and E) Detailed structural view of the interaction between two potential Furin inhibitors {2,5-dideoxystreptamine and peptide-based drug [succinyl-Phe-2-

https://dx.doi.org/10.1021/acs.jpclett.0c01698
J. Phys. Chem. Lett. 2020, 11, 6655−6663

Figure 2. continued

Nal-(Arg)3-Lys]-Lys-4-Amba} at the catalytic site of Furin. The position and residue names are labeled accordingly, and the type of interaction between the individual drug and amino acids is marked as shown in the legend.

The final docked complex structure was then compared with the initial Furin structure, and their overall RMSD was found to be 0.28 Å for Ca atoms. This suggests there are no large conformational changes upon docking. Interaction studies of potential drugs inhibiting Furin were performed in the Maestro software suite. All three-dimensional structures were visualized, and figures were generated using Pymol software.

The overall docked complex structure shows three Furin molecules binding to the mid or equatorial region (midregion of S1 and S2 domains, S1/S2) of the SARS-CoV-2 spike glycoprotein homotrimer at the adjacent side of the spike trimer (Figure 1B−D). Furin binding occurs in a clamp-like fashion, where it clips to the cleavage site of the spike glycoprotein. Furthermore, the binding of Furin protease creates a large burred interface of ∼970 Å^2/Furin between the proteins, as calculated from the PISA server (https://www.ebi.ac.uk/pdbe/pisa/). This suggests a bona fide and tight interaction of Furin protease over the spike glycoprotein and Furin. The depth, shape, and charge of Furin protease are well-known, and it has a canyon-like crevice. Its active site pocket is conserved in many species, where the catalytic or substrate-binding pocket is made of key amino acid residues R185, M189, D191, N192, R193, E229, V231, D233, D259, K261, R298, W328, and Q346[16,17] (Figure 2A). Interestingly, these residues are also well-positioned to interact with the viral spike protein cleavage site in our docked complex structure. The entire substrate-binding pocket of Furin protease appears like a canyon-like crevice, which can accommodate a large portion of the target protein/peptide. The docking results show that SARS-CoV-2 spike glycoprotein amino acid residues N657−Q690 are the prime residues interacting with the Furin protease. The position and orientation of these unique residues involved in Furin recognition are well-exposed. The spike protein residues N657, N658, E661, Y660, T678, N679, S680, R682, R683, R685, S689, and Q690 strongly interact with the Furin protease (Figure 2B).

The biophysical analysis shows that the interaction between the viral spike glycoprotein and Furin protease is mediated via several van der Waals bonds or hydrogen bonding. The entire cleavage loop or Furin site of viral spike protein fits and/or docks into the canyon-like substrate-binding pocket of Furin protease, which further corroborates the binding mode and orientation of Fuin over the spike glycoprotein. Furthermore, previous reports on the glycosylation of spike glycoprotein show that the Furin cleavage site in the SARS-CoV-2 spike glycoprotein is not targeted by glycosylation and this cleavage loop is completely solvent-exposed.[10] This validates the potential attack of Furin protease over the S1/S2 cleavage site. Furin modeled in complexes with potential Furin inhibitors {2,5-dideoxystreptamine and peptide-based drug [succinyl-Phe-2-Nal-(Arg)3-Lys]-Lys-4-Amba}[21,22] was also found to bind Furin protease with a higher affinity and shares the same conserved amino acid residues to interact with the proposed drugs (Figure 2D,E). This suggests that these drugs could potentially act by inhibiting Furin's interaction with the SARS-CoV-2 spike glycoprotein. The interaction between potential Furin inhibitors is mediated by several polar, hydrophobic, and salt-bridge interactions, which is consistent with the observed binding interactions between SARS-CoV-2 spike protein and Furin. The binding of these drugs also exhibits a very high affinity, and their ΔG values are −13 and −14.6 kcal, respectively, as estimated computationally. We next searched for other possible potential drugs or inhibitors[23] that could truly abolish the interaction with SARS-CoV-2 spike protein based on our complex binding mode, which is an addition to the action of a Furin inhibitor.

In this regard, we next looked at other potential known drugs or inhibitors of Furin and a related class of metalloproteases, which could potentially and structurally block the interaction between Furin and SARS-CoV-2 spike protein.[23−25] Some of these potential inhibitors are peptide-linked inhibitors such as Amba compounds, which have been observed previously to be effective in blocking the catalytic pocket of Furin.[21,22,24,26] Hence, we also analyzed the effectiveness of Amba compounds in blocking the interaction with SARS-CoV-2 spike protein individually. Among the various classes of inhibitors mentioned above, *m*-guanidinomethyl-Phac-RVR-Amba, H-Lys-Arg-Arg-Tle-Lys-4-Amba, c[glutaryl-BVK-Lys-Arg-Arg-Tle-Lys]-4-Amba, and *p*-guanidinomethyl-Phac-R-Tle-R-Amba were found to be most effective in blocking as they cover the larger surface area of the Furin in addition to its catalytic pocket. To corroborate that these drugs could structurally and functionally impede or abolish interaction with SARS-CoV-2 spike protein, we performed further docking studies with inhibitor-bound Furin with SARS-CoV-2 spike protein. As expected, we did not notice any interaction or complex formation with the Furin active pocket or at the cleavage site in spike protein (data not shown, as a result of the absence of complex formation). This suggests the effective abolishment of interaction with the SARS-CoV-2 spike protein. Binding of larger and cyclic inhibitors or drugs not only blocks the catalytic pocket of Furin but also masks the passive or noncatalytic sites that enhance or impede any passive or weak interaction with SARS-CoV-2 spike protein. This makes these longer peptide-linked inhibitors more competent and also stable as these inhibitors are linked with the stable peptide bond.[21,26] Interestingly, we also notice that cyclosporin drugs were also found to be potentially bind well to Furin.

On the contrary, smaller peptide-like inhibitors such as *N*-{2-methoxy-4-[(1-methylpiperidin-4-yl)oxy]phenyl}-4-(1*H*-pyrrolo[2,3-*c*]pyridin-3-yl)pyrimidin-2-amine, decanoyl-Arg-Val-Lys-Arg-chloromethylketone inhibitor, and *p*-guanidinomethyl-phenylacetyl-Arg-(3-methylvaline)-Arg-(amidomethyl) benzamidine were found to block the active site only, but this was sufficient to block Furin activity.[17,26] Virtual studies and superimposition of all of these competent drugs in Furin were also observed to effectively accommodate the large active pocket of Fuin, which further suggests its higher potency. In this regard, it has been demonstrated that different peptide-linked inhibitors such as Amba compounds have been used as a potential inhibitors.[21,23,25] These observations of drug binding and blocking the function of Furin and their efficacy at impeding the interaction with SARS-CoV-2 spike protein warrant further preclinical and future clinical studies.

We next looked at the artificially inserted and engineered Furin cleavage site in the SARS-CoV-1 spike glycoprotein that showed cleavage of spike protein into S1 and S2 domains in the

https://dx.doi.org/10.1021/acs.jpclett.0c01698
J. Phys. Chem. Lett. 2020, 11, 6655−6663

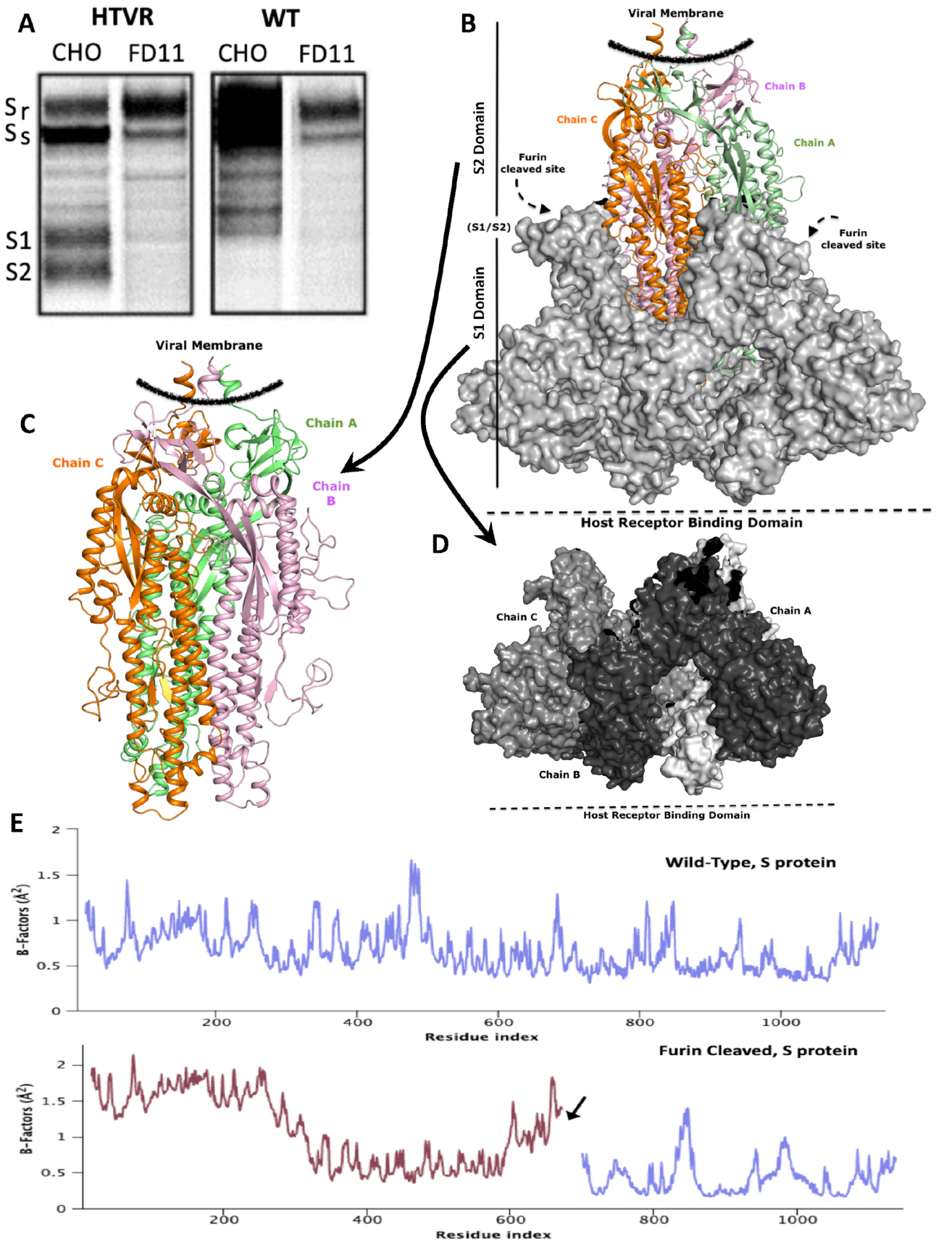

Figure 3. (A) Proteolytic processing in natural Chinese hamster ovary cells and FD11 (Furin-deficient) cells. Wild-type (WT) spike glycoprotein and the Furin site-containing engineered spike glycoprotein (HTVR). The S glycoprotein in cell lysates was affinity isolated. The Endo-H-resistant (Sr) and Endo-H-sensitive (Ss) forms of the S glycoprotein are indicated. The cleaved S1 and S2 polypeptide fragments are denoted and consistent with a molecular weight with cleavage in the S1/S2 junction region. Figure adapted and modified from ref 18. (B) Structural interpretation after Furin

https://dx.doi.org/10.1021/acs.jpclett.0c01698
J. Phys. Chem. Lett. 2020, 11, 6655−6663

Figure 3. continued

cleavage in the S1/S2 junction region of SARS-CoV-2 spike glycoprotein. Surface (S1 domains) and cartoon (S2 domains) representation showing the cleaved and separated structures of S1 and S2 domains after Furin cleavage. (C) Three monomers of the SARS-CoV-2 spike glycoprotein homotrimer of S2 domains colored green (chain A), pink (chain B), and orange (chain C). (D) Surface representation of the S1 domains shown in shades of gray. (E) Molecular dynamics simulation studies showing the oscillation and *B*-factor profiles of wild-type and Furin-cleaved SARS-CoV-2 spike glycoprotein. The amino acid residue position is shown on the *X*-axis, and the degree of movement of amino acids as the *B*-factor is shown on the *Y*-axis.

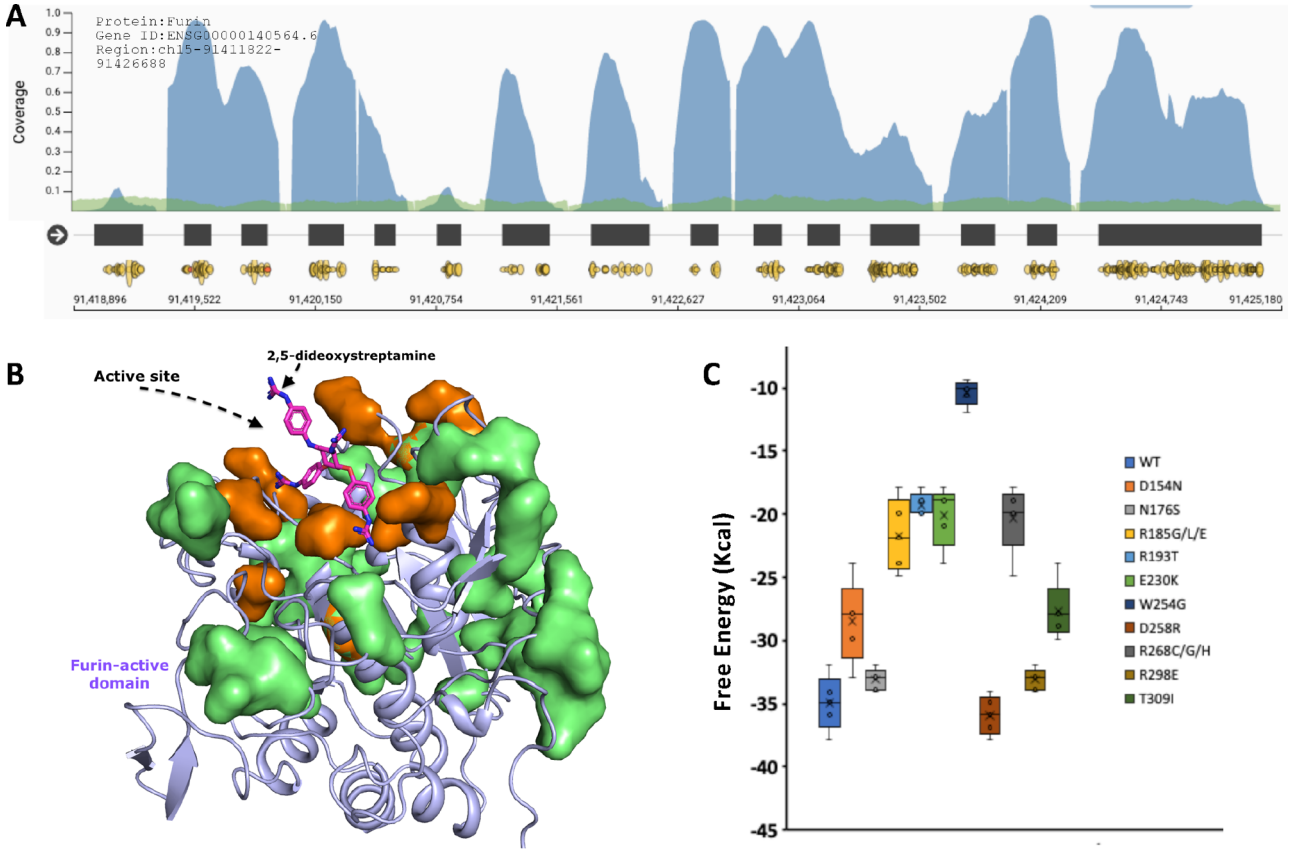

D

rsID	Amino Acid and NT Variant		Variant type	Allele Frequency	rsID	Amino Acid and NT Variant		Variant type	Allele Frequency
rs1246114763	Asp154Asn	460G>A	missense	3.9776E-06	rs770393100	Asp58Arg	802C>G	missense	4.0577E-06
rs1432327819	Asn176Ser	527A>G	missense	4.0051E-06	rs188842168	Trp245Gly	734T>G	missense	1.5932E-05
rs763052854	Arg185Trp	553C>T	missense	4.0333E-06	rs770393100	Arg268Cys	802C>T	missense	8.1153E-06
rs763052854	Arg185Gly	553C>G	missense	4.0333E-06	rs770393100	Arg268Gly	802C>G	missense	4.0577E-06
rs1282092505	Arg185Leu	554G>T	missense	4.0417E-06	rs199849515	Arg268His	803G>A	missense	2.4427E-05
rs1282092505	Arg185Gln	554G>A	missense	4.0417E-06	rs769208985	Arg298Gln	893G>A	missense	8.025E-06
rs760668224	Arg193Thr	578G>C	missense	4.1573E-06	rs774662648	Glu299Lys	895G>A	missense	4.0101E-06
rs1347562753	Glu230Lys	688G>A	missense	3.9864E-06	rs1178982886	Thr309Ile	926C>T	missense	1.2011E-05

Figure 4. (A) Genome (green) and exome (blue peaks) regions of Furin on human chromosome 15. The transcripts are shown in the black boxes, and yellow dots indicate the overserved mutations or SNPs or genetic variations. The sequence region is labeled. (B) Structure of the Furin protease (active or catalytic domain) as a blue ribbon model, with observed missense mutations found in the exome sequencing shown as green (noncatalytic pocket residues) and orange (residues involved in drug and spike protein interaction) surface patches. (C) The effect of human genetic mutations or variant alleles in the catalytic pocket of Furin alters the binding free energy (kilocalories) with SARS-CoV-2 spike protein. Each genetic variant and its respective binding free energy with spike protein are shown. (D) Table of missense mutations and their positions and SNP IDs.

presence of Furin protease, when tested in Chinese hamster ovary (CHO) cells (Figure 3),[18,27] whereas the Furin protease knockout CHO cells showed no cleavage of spike glycoprotein. This is consistent with the absence of a Furin site in the SARS-CoV-1 spike glycoprotein, which is resistant to Furin protease (Figure 3A). On the basis of the structural, functional, and biophysical observations of Furin binding, we structurally showed that the binding and cleaving (priming) of the SARS-CoV-2 spike glycoprotein in the S1/S2 region by Furin protease result in the separation of the N-terminal S1 domain (Figure 3B,D) (Movie S1) involved in host cell recognition (interact with ACE2 or CD26) and C-terminal S2 membrane-anchored domain (Figure 3A,C) involved in host cell penetration and entry (may involve in the interaction with other proteases such as TMPRSS2). In support of this supposition, the presence of the Furin cleavage site in infectious bronchitis virus has

https://dx.doi.org/10.1021/acs.jpclett.0c01698
J. Phys. Chem. Lett. 2020, 11, 6655−6663

pronounced virulence,[28] suggesting Furin cleavage increases virulence.[13,29] Hence, the presence of Furin sites in the spike glycoprotein is a hallmark of enhanced virulence, thus making SARS-CoV-2 a highly virulent strain.

To validate this hypothesis, we performed virtual biophysical experiments using molecular dynamics and simulations for the SARS-CoV-2 spike protein and Furin protease complex structure employed the servers DynOmics (www.gnm.csb.pitt.edu)[30] and LARMD (www.chemyang.ccnu.edu). The time course simulations at 10 ns were recorded. *B*-Factor profiles and domain separation analysis combined with simulation studies were performed using the DynOmics server and validated with Schrodinger molecular dynamics tertiaries. Our extended biophysical molecular dynamics and simulation studies also suggest that the cleavage of spike glycoprotein in the S1/S2 region (Figure S1 and Movies S2 and S3) decreased the stability of the S1 domains of the protein, suggesting the possible separation of domains. These observations were further substantiated with extended molecular dynamics and simulation studies to address the flexibility of domains with respect to the cleavage of spike protein by Furin (Figure 3E and Figure S3). It is evident from the molecular dynamics that the wild-type protein possesses a low *B*-factor (stability factor, where a lower number indicates greater stability) but the N-terminal domain *B*-factor drastically increases with the cleavage action by Furin (Figure 3E). Increases in *B*-factors were also directly linked with the domain superstation as the complex structure is thermodynamically unstable and considerably flexible, which will cause Furin and the spike protein to separate. Hence, we next sought to check the domain separation action in response to Furin cleavage through biophysical and time course eigenvectors (separation dynamics). As shown in Figure S3, abrupt and higher eigenvectors were observed at the N-terminal (S1) domains. Increased eigenvectors are directly linked with domain separation, whereas the C-terminal (S2) domain maintains low eigenvectors and provides a high degree of confidence for retaining a stable homotrimer structure as shown in Figure 3C.

Due to the enzymatic cleavage and separation of the S1 and S2 domains, the inhibitors for ACE2 may be least effective and host receptors are not required for further cell penetration. This also raises the point that these cleavage activities need to be considered with respect to the production of neutralizing antibodies targeting SARS-CoV-2 spike glycoprotein. This makes SARS-CoV-2 more virulent, and previously existing antibodies or ACE2 inhibitors are not highly effective against the virus. This study is also the first to show biophysically and structurally how human Furin interacts with the coronavirus spike glycoprotein, which underlines its mechanism of action. This structural and molecular dynamics study has great implications for the further development of Furin protease inhibitors, to block the protease activity of Furin and too aid in the development of bona fide antibodies targeting the S1/S2 Furin cleavage site of spike glycoprotein, which warrant further clinical investigation.

On the contrary, the gene expression levels and profile of an enzyme provide the possible infection target region and its severity. We first looked at the endogenous gene expression levels of Furin from human isolates from different parts of the body (Figure S5A). As expected, higher levels of Furin expression were found in the lungs and liver. Furthermore, elevated levels of expression were also found in the prostate gland (Figure S3A), which may have implications for the greater susceptibility of men versus women as noticed from the different epidemiological studies in which more men are infected with SARS-CoV-2.[31,32] Similarly, we also looked into the expression profiles under different cancer conditions (Figure S5B), which underlines the importance of Furin not only in relation to viral infection but also for different disease conditions. This also warrants further studies of the expression levels with respect to genetic variations or alleles in humans. The presence of alleles or genetic variations is directly linked to altered infections in humans due to its different binding to target virulent proteins.[33] Such genetic variants or alleles were also found with HIV, malaria, and other infections, leading to a different resistance or infection rate.[34,35]

To unravel the genetic variants in human Furin and to understand the possible differences in virulence, we performed whole-exome sequencing analysis of Furin protease from the sequencing data of nearly 40000 human individuals derived from next-generation sequencing data from the GTIxp portal and GenomeAD V3.1 repository.[36,37] The exome sequence data were filtered to extract only missense mutations that occurred in the whole exome of human Furin encoded on chromosome 15. All missense and deleterious mutations/SNPs or genetic alleles or variants are tabulated for further structural and binding analyses. The gene encoding Furin is located on chromosome 15 and stretches from the region 91,418,869 to 91,425,180 (containing both exome and genome regions) (Figure 4A). It was surprising to notice from the genome sequence alignment of Furin among the 40000 human individuals, several hundred genetic variants or alleles were found in Furin (Figure 4A and Table 1 of the Supporting Information). However, most of the variants were synonymous (no change in the amino acid sequence), and nearly 160 SNPs or alleles are missense and nonsense variants. Among all of these alleles or variants, 11 variants were found to be located in the active site or catalytic pocket of Furin (Figure 4C,D), which is directly involved in the interaction with the target SARS-CoV-2 spike protein or any candidate drug that could block Furin activity and impede further biophysical processes. Furthermore, the allele frequency was also high, suggesting its presence in a large proportion of the population (Figure 4D).

To test the significance of the variants in binding SARS-CoV-2 spike protein, we performed binding energy calculations virtually by mutating individual amino acid residues and docked or simulated the structures to measure the overall binding free energy (kilocalories) in the presence of SARS-CoV-2 spike protein. As shown in Figure 4B, in the structure of Furin protease, the key residues involved in the interaction or catalytic pocket (highlighted as an orange surface) are completely surrounded and directed to the site. The binding kinetics and biophysical characterization show that wild-type Furin binds to spike protein with a free energy of −37 kcal and most of the mutants showed a significant decrease in binding affinity with the spike protein (Figure 4C). Among the different mutations, the most significant genetic variant was found to be W254G. With a calculated binding free energy of −11 kcal, this indicates a >3-fold decrease in binding affinity (Figure 4C). The decrease in binding affinity can be directly correlated with the decrease in the extent of viral infection, as the action of Furin over the spike protein will be limited. Unravelling the genetic mutations and their binding affinities underlines the significance of the development of therapeutics and of understanding the genome variation leading to differential infection rates, which warrants further clinical studies.

https://dx.doi.org/10.1021/acs.jpclett.0c01698
J. Phys. Chem. Lett. 2020, 11, 6655−6663

Similarly, the rate and number of SNPs or mutations in SARS-CoV-2 within five months of the initial outbreak underline the complexity of the quick evolution of SARS-CoV-2. As human Furin targets SARS-CoV-2 spike protein, the mutations or SNPs are surface-exposed, and in the solvent-accessible regions, some are involved in host receptor (ACE2 and CD26)[10,14,20] binding and to a minor extent in the Furin cleavage site (Figures S6 and S7). However, how these mutations influence the pathogenicity and virulence is elusive and requires further investigation. Most of the mutations observed are "missense" SNPs or variants in the adjacent loop region (not the neighboring amino acids) of the Furin-binding site of the SARS-CoV-2 spike protein (Figures S6 and S7), which might be passively involved in building an interface with Furin. These mutations could impact virulence and could contribute to resistance toward inhibitors or antibodies. However, some of these mutations were found to revert over the time course. We also note that no mutations were observed at the Furin cleavage site or the neighboring amino acids, making the spike protein still susceptible to cleavage by the action of Furin. This warrants the use of abundant caution by the medical fraternity and pharmacologists in using antivirals and antibodies and the need to screen which drugs are compatible and promising with respect to their respective SARS-CoV-2 variant for treatment.

In conclusion, our structural docking, biophysical analysis, and molecular dynamics studies demonstrate that human Furin protease binds to SARS-CoV-2 spike protein with high affinity (−37 kcal) and cleaves the viral spike protein into S1 and S2 domains. The drug docking analysis demonstrated that 2,5-dideoxystreptamine and the peptide-based drug [succinyl-Phe-2-Nal-(Arg)3-Lys]-Lys-4-Amba bind to Furin with high affinity (−13 kcal), establishing various hydrogen bonds and polar and hydrophobic interactions, and these may act as potential antiviral drugs against SARS-CoV-2. Furthermore, the unravelling of the genetic variants of Furin in humans and the binding affinities of Furin for target viral protein highlights the role and protection mechanism of viral infection. Unravelling the structure and understanding the binding mechanism of Furin protease, drug molecules, and genetic variants in host Furin and SNPs in SARS-CoV-2 may assist in the development of potential therapeutics or drug molecules to efficiently target SARS-CoV-2. Moreover, the structural analysis and detailed interaction map provide deeper insight and encourage further drug development studies.

■ ASSOCIATED CONTENT

Supporting Information

The Supporting Information is available free of charge at https://pubs.acs.org/doi/10.1021/acs.jpclett.0c01698.

Multiple-sequence alignment of SARS-CoV-2 and SARS-CoV-1 spike glycoproteins, validation report for the predicted structure of Furin in complex with SARS-CoV-2 spike glycoprotein, domain separation dynamics of cleaved SARS-CoV-2 spike glycoprotein by Furin, sructural interaction of Furin with other potential inhibitors of Furin, tissue specific protein expression level of human Furin protease, time course mutations and changes in SARS-CoV-2, and missense amino acid mutations obversed in the spike glycoprotein over time in different countries (PDF)

Structural overview of the interaction of Furin protease with SARS-CoV-2 spike glycoprotein and its cleavage action (MP4)

Dynamic simulation and stability of native spike glycoprotein (MOV)

Dynamic simulation and stability of Furin-cleaved spike glycoprotein (MOV)

Supplemental table (XLSX)

■ AUTHOR INFORMATION

Corresponding Author

Naveen Vankadari − *Monash Biomedicine Discovery Institute and Department of Biochemistry and Molecular Biology, Monash University, Victoria 3800, Australia;* orcid.org/0000-0001-9363-080X; Phone: +61 03 99029229; Email: Naveen.vankadari@monash.edu

Complete contact information is available at: https://pubs.acs.org/10.1021/acs.jpclett.0c01698

Notes

The author declares no competing financial interest.

■ ACKNOWLEDGMENTS

I thank the Monash University Software Platform for licence access to the software. I also acknowledge Joseph Polidano of the University of Melbourne for language editing and proofreading the manuscript. The Furin protease cleavage gel pictures adopted with licence number 4818611148181 for use in this publication. I thank NGDC (www.bigd.big.ac.cn/) for giving permission and agreement for the use of the sequencing data and graphical images used. Gene expression data were obtained from the Gent2 repository (www.gent2.com).

■ REFERENCES

(1) Huang, C.; Wang, Y.; Li, X.; Ren, L.; Zhao, J.; Hu, Y.; Zhang, L.; Fan, G.; Xu, J.; Gu, X.; et al. Clinical features of patients infected with 2019 novel coronavirus in Wuhan, China. *Lancet* **2020**, *395* (10223), 497−506.

(2) Vankadari, N. Overwhelming Mutations or SNPs of SARS-CoV-2: A Point of Caution. *Gene* **2020**, *752*, 144792.

(3) Zhang, J.; Zhou, L.; Yang, Y.; Peng, W.; Wang, W.; Chen, X. Therapeutic and triage strategies for 2019 novel coronavirus disease in fever clinics. *Lancet Respir. Med.* **2020**, *8* (3), e11−e12.

(4) Li, G.; De Clercq, E. Therapeutic options for the 2019 novel coronavirus (2019-nCoV). *Nat. Rev. Drug Discovery* **2020**, *19* (3), 149−150.

(5) Amawi, H.; Abu Deiab, G. I.; A Aljabali, A. A.; Dua, K.; Tambuwala, M. M. COVID-19 pandemic: an overview of epidemiology, pathogenesis, diagnostics and potential vaccines and therapeutics. *Ther. Delivery* **2020**, *11* (4), 245−268.

(6) Vankadari, N. Arbidol: A potential antiviral drug for the treatment of SARS-CoV-2 by blocking trimerization of the spike glycoprotein. *Int. J. Antimicrob. Agents* **2020**, 105998.

(7) Zhou, P.; Yang, X. L.; Wang, X. G.; Hu, B.; Zhang, L.; Zhang, W.; Si, H. R.; Zhu, Y.; Li, B.; Huang, C. L.; et al. A pneumonia outbreak associated with a new coronavirus of probable bat origin. *Nature* **2020**, *579* (7798), 270−273.

(8) Xu, X.; Chen, P.; Wang, J.; Feng, J.; Zhou, H.; Li, X.; Zhong, W.; Hao, P. Evolution of the novel coronavirus from the ongoing Wuhan outbreak and modeling of its spike protein for risk of human transmission. *Sci. China: Life Sci.* **2020**, *63*, 457−460.

(9) Walls, A. C.; Park, Y. J.; Tortorici, M. A.; Wall, A.; McGuire, A. T.; Veesler, D. Structure, Function, and Antigenicity of the SARS-CoV-2 Spike Glycoprotein. *Cell* **2020**, *181*, 281−292.e6.

(10) Vankadari, N.; Wilce, J. A. Emerging WuHan (COVID-19) coronavirus: glycan shield and structure prediction of spike glycoprotein and its interaction with human CD26. *Emerging Microbes Infect.* **2020**, *9* (1), 601−604.
(11) Li, Y.; Zhang, Z.; Yang, L.; Lian, X.; Xie, Y.; Li, S.; Xin, S.; Cao, P.; Lu, J. The MERS-CoV receptor DPP4 as a candidate binding target of the SARS-CoV-2 spike. *iScience* **2020**, *23*, 101160.
(12) Andersen, K. G.; Rambaut, A.; Lipkin, W. I.; Holmes, E. C.; Garry, R. F. The proximal origin of SARS-CoV-2. *Nat. Med.* **2020**, *26*, 450−452.
(13) Hasan, A.; Paray, B. A.; Hussain, A.; Qadir, F. A.; Attar, F.; Aziz, F. M.; Sharifi, M.; Derakhshankhah, H.; Rasti, B.; Mehrabi, M.; Shahpasand, K.; Saboury, A. A.; Falahati, M. A review on the cleavage priming of the spike protein on coronavirus by angiotensin-converting enzyme-2 and furin. *J. Biomol. Struct. Dyn.* **2020**, 1−13.
(14) Coutard, B.; Valle, C.; de Lamballerie, X.; Canard, B.; Seidah, N. G.; Decroly, E. The spike glycoprotein of the new coronavirus 2019-nCoV contains a furin-like cleavage site absent in CoV of the same clade. *Antiviral Res.* **2020**, *176*, 104742.
(15) de Greef, J. C.; Slutter, B.; Anderson, M. E.; Hamlyn, R.; O'Campo Landa, R.; McNutt, E. J.; Hara, Y.; Pewe, L. L.; Venzke, D.; Matsumura, K.; et al. Protective role for the N-terminal domain of alpha-dystroglycan in Influenza A virus proliferation. *Proc. Natl. Acad. Sci. U. S. A.* **2019**, *116* (23), 11396−11401.
(16) Dahms, S. O.; Arciniega, M.; Steinmetzer, T.; Huber, R.; Than, M. E. Structure of the unliganded form of the proprotein convertase furin suggests activation by a substrate-induced mechanism. *Proc. Natl. Acad. Sci. U. S. A.* **2016**, *113* (40), 11196−11201.
(17) Henrich, S.; Cameron, A.; Bourenkov, G. P.; Kiefersauer, R.; Huber, R.; Lindberg, I.; Bode, W.; Than, M. E. The crystal structure of the proprotein processing proteinase furin explains its stringent specificity. *Nat. Struct. Mol. Biol.* **2003**, *10* (7), 520−6.
(18) Follis, K. E.; York, J.; Nunberg, J. H. Furin cleavage of the SARS coronavirus spike glycoprotein enhances cell-cell fusion but does not affect virion entry. *Virology* **2006**, *350* (2), 358−69.
(19) Eden, J. S.; Rockett, R.; Carter, I.; Rahman, H.; de Ligt, J.; Hadfield, J.; Storey, M.; Ren, X.; Tulloch, R.; Basile, K.; et al. An emergent clade of SARS-CoV-2 linked to returned travellers from Iran. *Virus Evol.* **2020**, *6* (1), veaa027.
(20) Wrapp, D.; Wang, N.; Corbett, K. S.; Goldsmith, J. A.; Hsieh, C. L.; Abiona, O.; Graham, B. S.; McLellan, J. S. Cryo-EM structure of the 2019-nCoV spike in the prefusion conformation. *Science* **2020**, *367* (6483), 1260−1263.
(21) Van Lam van, T.; Ivanova, T.; Hardes, K.; Heindl, M. R.; Morty, R. E.; Bottcher-Friebertshauser, E.; Lindberg, I.; Than, M. E.; Dahms, S. O.; Steinmetzer, T. Design, Synthesis, and Characterization of Macrocyclic Inhibitors of the Proprotein Convertase Furin. *ChemMedChem* **2019**, *14* (6), 673−685.
(22) Dahms, S. O.; Jiao, G. S.; Than, M. E. Structural Studies Revealed Active Site Distortions of Human Furin by a Small Molecule Inhibitor. *ACS Chem. Biol.* **2017**, *12* (5), 1211−1216.
(23) Couture, F.; Kwiatkowska, A.; Dory, Y. L.; Day, R. Therapeutic uses of furin and its inhibitors: a patent review. *Expert Opin. Ther. Pat.* **2015**, *25* (4), 379−96.
(24) Dahms, S. O.; Hardes, K.; Becker, G. L.; Steinmetzer, T.; Brandstetter, H.; Than, M. E. X-ray structures of human furin in complex with competitive inhibitors. *ACS Chem. Biol.* **2014**, *9* (5), 1113−8.
(25) Braun, E.; Sauter, D. Furin-mediated protein processing in infectious diseases and cancer. *Clin. Transl. Immunol.* **2019**, *8* (8), No. e1073.
(26) Hardes, K.; Becker, G. L.; Lu, Y.; Dahms, S. O.; Kohler, S.; Beyer, W.; Sandvig, K.; Yamamoto, H.; Lindberg, I.; Walz, L.; Steinmetzer, T.; et al. Novel Furin Inhibitors with Potent Anti-infectious Activity. *ChemMedChem* **2015**, *10* (7), 1218−31.
(27) Hasan, A.; Paray, B. A.; Hussain, A.; Qadir, F. A.; Attar, F.; Aziz, F. M.; Sharifi, M.; Derakhshankhah, H.; Rasti, B.; Mehrabi, M.; et al. review on the cleavage priming of the spike protein on coronavirus by angiotensin-converting enzyme-2 and furin. *J. Biomol. Struct. Dyn.* **2020**, 1−9.
(28) Yamada, Y.; Liu, D. X. Proteolytic activation of the spike protein at a novel RRRR/S motif is implicated in furin-dependent entry, syncytium formation, and infectivity of coronavirus infectious bronchitis virus in cultured cells. *J. Virol.* **2009**, *83* (17), 8744−58.
(29) Le Coupanec, A.; Desforges, M.; Meessen-Pinard, M.; Dube, M.; Day, R.; Seidah, N. G.; Talbot, P. J. Cleavage of a Neuroinvasive Human Respiratory Virus Spike Glycoprotein by Proprotein Convertases Modulates Neurovirulence and Virus Spread within the Central Nervous System. *PLoS Pathog.* **2015**, *11* (11), No. e1005261.
(30) Li, H.; Chang, Y. Y.; Lee, J. Y.; Bahar, I.; Yang, L. W. DynOmics: dynamics of structural proteome and beyond. *Nucleic Acids Res.* **2017**, *45* (W1), W374−W380.
(31) McCoy, J.; Wambier, C. G.; Vano-Galvan, S.; Shapiro, J.; Sinclair, R.; Muller Ramos, P.; Washenik, K.; Andrade, M.; Herrera, S.; Goren, A. Racial Variations in COVID-19 Deaths May Be Due to Androgen Receptor Genetic Variants Associated with Prostate Cancer and Androgenetic Alopecia. Are Anti-Androgens a Potential Treatment for COVID-19? *J. Cosmet., Dermatol. Sci. Appl.* **2020**, *19*, 1542.
(32) Jin, J. M.; Bai, P.; He, W.; Wu, F.; Liu, X. F.; Han, D. M.; Liu, S.; Yang, J. K. Gender Differences in Patients With COVID-19: Focus on Severity and Mortality. *Front. Public Health* **2020**, *8*, 152.
(33) Burgner, D.; Jamieson, S. E.; Blackwell, J. M. Genetic susceptibility to infectious diseases: big is beautiful, but will bigger even better? *Lancet Infect. Dis.* **2006**, *6* (10), 653−63.
(34) Hedrick, P. W. Population genetics of malaria resistance in humans. *Heredity* **2011**, *107* (4), 283−304.
(35) An, P.; Winkler, C. A. Host genes associated with HIV/AIDS: advances in gene discovery. *Trends Genet.* **2010**, *26* (3), 119−31.
(36) Lek, M.; Karczewski, K. J.; Minikel, E. V.; Samocha, K. E.; Banks, E.; Fennell, T.; O'Donnell-Luria, A. H.; Ware, J. S.; Hill, A. J.; Cummings, B. B.; et al. Exome Aggregation, C. Analysis of protein-coding genetic variation in 60,706 humans. *Nature* **2016**, *536* (7616), 285−91.
(37) Carithers, L. J.; Moore, H. M. The Genotype-Tissue Expression (GTEx) Project. *Biopreserv. Biobanking* **2015**, *13* (5), 307−8.

https://dx.doi.org/10.1021/acs.jpclett.0c01698
J. Phys. Chem. Lett. 2020, 11, 6655−6663